Centribuoyancy in a Causal Null-History Field

Stress-Moment Closure, the General-Relativistic Limit, and One-Ended BECOs

Esa Sakkinen

Independent researcher in the ΦBSU programme, Finland

August 2026

Abstract

This article formulates *centribuoyancy* as the outward physical acceleration of a causal null-history field whose inward gravitational appearance is an operational coordinate projection. The construction reverses the classical centrifugal relation twice: the direction of the real effect changes and its carrier moves from a material binding to the field itself. The invariant total four-density ρ_Φ and its spatial projection $\rho_\perp$ are assigned opposite profiles around a closed matter centre, so that one orientation conversion supplies both an outward field acceleration and inward coordinate gravity without a sign contradiction.

The field stress is constructed from a local moment hierarchy of null histories. Every diagonal second moment of individual null momenta is identically trace-free; invariant mass and the nonzero trace arise only from non-diagonal correlations in closed history classes. The total history-medium stress is then separated into a geometrized equilibrium component and an excitation component. The former is encoded once in the operational coframe and must not be counted again as a source; the latter contains finite-memory, finite-size, tidal, self-force and radiative residues. Consequently, freely falling and freely orbiting point bodies have zero proper acceleration, while distributed field momentum remains physical.

A local general-relativistic limit is obtained conditionally. Lovelock uniqueness applies only when the short-memory coincidence response factors through the operational metric, with no independent closure or history invariant surviving beside it. Under that condition the static isotropic sector yields $\gamma_{\text{PPN}} = \beta_{\text{PPN}} = 1$; conversely, gravitational slip or additional polarizations test failure of the same factorization. The full history-to-coframe map contains lapse, shift and an independent unimodular spatial sector. Its trace-free screen shear supplies the two tensor gravitational-wave degrees of freedom; these modes vanish in the conformastatic scalar special case rather than being generated by it.

The exponential metric is recovered as the static isotropic exterior chart. Its global two-ended continuation is retained only as a general-relativistic comparison. The physical buoyant exotic compact object (BECO) is a one-ended nonlinear history closure with finite proper volume. The exterior photon orbit lies at isotropic $r = 2m$, outside the areal-map fold at $r = m$, so the critical impact parameter $b_{\text{crit}} = 2em$ remains an exterior prediction whenever nonlinear closure begins inside $2m$.

Keywords: null congruence; causal memory; stress-energy moments; general-relativistic limit; gravitational radiation; compact objects; PPN; quasilocal momentum.

Assumptions and scope. Exact influence is local and is transported along neighbouring null histories. The history measure, its open–closed conversion operator and the nonlinear BECO core are constitutive objects to be derived from the primary action. Algebraic moment identities, the stated weak-field expansion and the exterior exponential-chart identities are direct consequences of the definitions used here. The local Einstein closure is a conditional result: it requires metric factorization of the coincidence response. If an independent closure scalar, vector or tensor survives that limit, the theory belongs to a broader scalar/vector-tensor class and must be tested as such. The global wormhole continuation of the exponential line element is a comparison geometry, not the assumed physical topology.

1. Introduction: the centrifugal analogy, inverted

Consider a mass constrained to forced circular motion. The physically real interaction is the inward binding that turns the velocity vector,

$$\mathbf{F}_{\text{bind}} = -M\frac{v^2}{R}\,\hat{\mathbf{r}}, \tag{1}$$

whereas the outward centrifugal force

$$\mathbf{F}_{\mathrm{cf}} = +M\frac{v^2}{R}\,\hat{\mathbf{r}} \tag{2}$$

appears only when the same motion is written in the co-rotating chart. A fictitious force cannot serve as the physical source of the chart that generates it.

The proposed gravitational relation is the mirror image. The real acceleration belongs to the null-history field and points outward from the local curvature centre; the inward gravitational acceleration belongs to the operational coordinate map. The analogy is therefore not a single sign flip. Both direction and ontological carrier change, as shown in fig. 1.

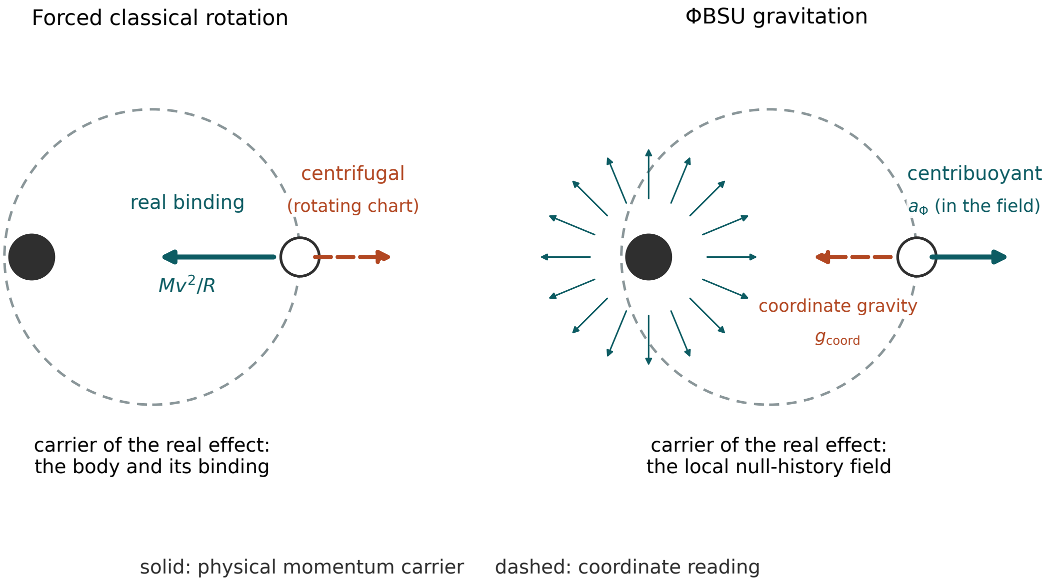

Figure 1. The double swap. In forced rotation the real inward binding acts on the body and the outward effect is coordinate. In the ΦBSU reading the real outward acceleration resides in the local null-history field and the inward gravitational effect is the coordinate shadow.

The claim is not that an outward force is added to an inward gravitational force. It is that the same physical structure has an outward field reading and an inward coordinate reading. Proper force on matter is a third question, treated separately below.

The article develops this claim as a field-theory construction rather than as a verbal analogy. Its technical steps are: a causal null-history state, a moment construction of field stress, a no-double-counting split between geometrized equilibrium and excitation stress, a conditional local-GR theorem, a general coframe sector carrying rotation and tensor radiation, and a one-ended strong-field BECO boundary problem. The operational metric remains a chart of the field state, in continuity with the Separverse programme of Part I [1]; standard GR is recovered only on the domain where the history closure becomes local and metric-factorized.

2. Phase field, four-density and physical field acceleration

Let the global phase be

$$\Phi = e^{i\alpha}, \qquad q = \mathrm{d}\alpha. \tag{3}$$

The one-form q is metric-free. The exact theory requires its norm to be defined in the primary separative coframe rather than by assuming the operational metric in advance. Denote that constitutive norm by

$$\rho_\Phi^2 = \left|\mathfrak{G}^{AB}[\mathcal{H}]\,Q_A Q_B\right|, \qquad Q_A = E_A{}^{\mu}\mathcal{D}_\mu\alpha, \tag{4}$$

where $E_A{}^{\mu}$ is a primary coframe and $\mathfrak{G}^{AB}$ is determined by the local null-history state. In the local GR closure this reduces to the familiar shorthand

$$\rho_\Phi = \sqrt{|g_{\rm op}^{\mu\nu} q_\mu q_\nu|}. \tag{5}$$

Thus no metric is smuggled into the ontology through the definition of the field whose projection later generates that metric.

Throughout the article, $\mathcal{D}_\mu$ denotes the primary/history-covariant derivative before operational coframe closure, $\nabla_\mu^{\rm op}$ the Levi–Civita derivative of $g_{\mu\nu}^{\rm op}$ after that closure, and ∂_μ ordinary differentiation of scalar components in a chosen chart. For the first derivative of a scalar these agree in a fixed chart; the separate symbols record the layer at which the derivative is being used.

Define the dimensionless orientation-conversion potential and the covariant buoyancy gradient

$$\chi_\Phi = \ln\left(\frac{\rho_\Phi}{\rho_{\Phi,\infty}}\right), \qquad b_\mu = -\mathcal{D}_\mu \chi_\Phi. \tag{6}$$

The corresponding SI acceleration scale is

$$a_{\Phi\mu} = c^2 b_\mu = -c^2 \mathcal{D}_\mu \chi_\Phi. \tag{7}$$

Equation (7) is first a field covector. Raising its index requires the constitutive inverse of the local coframe; in the operational closure this is $g_{\rm op}^{\mu\nu}$.

For a local screen projector $P_\perp$, define the primitive field-curvature scale

$$\boldsymbol{\kappa}_\Phi^{\rm field} = -P_\perp \mathcal{D}\chi_\Phi, \qquad P_\perp \mathbf{a}_\Phi = c^2 \boldsymbol{\kappa}_\Phi^{\rm field}. \tag{8}$$

The factor c^2 is the ordinary kinematic factor for a curvature form transported at c; it contains no additional numerical factor two. The factor two belongs to the operational null-geodesic projection and is derived in section 8.

At roughly 1000 km above the Earth's surface, $g \simeq 7.34\,\mathrm{m\,s^{-2}}$. The corresponding one-projection field curvature is

$$|\kappa_\Phi^{\rm field}| \simeq \frac{7.34}{c^2} \simeq 8.17 \times 10^{-17}\ \mathrm{m}^{-1}, \qquad \mathcal{R}_\Phi^{\rm field} \simeq 1.22 \times 10^{16}\ \mathrm{m} \simeq 1.29\ \mathrm{ly}. \tag{9}$$

This is not an orbital radius. It is a local curvature scale: a nearly straight c-transported bundle can manifest ordinary gravity because the transport speed is extreme.

3. Two branches: total four-density and spatial projection

A single density symbol is insufficient once the mass term, the outward field acceleration and the inward spatial reading are discussed together. Relative to an operational observer U^μ, decompose

$$q^\mu = q_\parallel^\mu + q_\perp^\mu, \qquad q_\parallel^\mu = -\frac{q_\nu U^\nu}{c^2} U^\mu, \qquad q_\perp^\mu = h^\mu{}_\nu q^\nu, \tag{10}$$

with

$$\rho_\parallel = \frac{|U^\mu q_\mu|}{c}, \qquad \rho_\perp = \sqrt{h^{\mu\nu} q_\mu q_\nu}. \tag{11}$$

Matter closure rotates the dominant orientation toward the proper-time branch,

$$\Delta\left(\frac{\rho_\parallel}{\rho_\perp}\right) > 0. \tag{12}$$

The invariant total norm can therefore increase toward a closed matter centre while the spatially readable branch is depleted there.

On the static, single-source, optically conserved branch the exchange law is

$$\mathrm{d}\ln\rho_\perp = -\mathrm{d}\ln\rho_\Phi. \tag{13}$$

With the radial unit vector pointing outward,

$$\partial_r\rho_\Phi < 0, \qquad \partial_r\rho_\perp > 0, \tag{14}$$

and hence

$$\mathbf{a}_\Phi = -c^2\boldsymbol{\nabla}^{\mathrm{op}}\ln\rho_\Phi \quad \text{is outward}, \qquad \mathbf{g}_{\mathrm{coord}} = -c^2\boldsymbol{\nabla}^{\mathrm{op}}\ln\rho_\perp = -\,\mathrm{proj}_3\,\mathbf{a}_\Phi \quad \text{is inward}. \tag{15}$$

There is no sign reversal inside one scalar. The two signs arise from two projections of one orientation conversion. Figure 2 displays the static profile $\chi = m/r$.

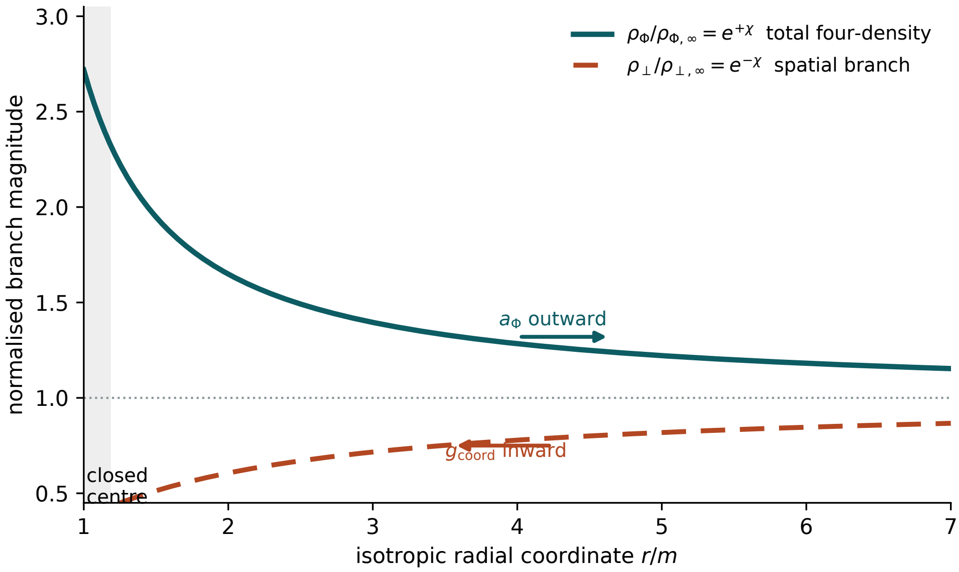

Figure 2. The total and spatial branches for $\chi = m/r$. A closed matter centre is a maximum of total four-density and a depletion of the spatial branch. The reciprocity relation is a constitutive statement for the static observer family, not a general observer-independent identity.

The decomposition is observer-dependent because U^μ is. In this note the explicit radial formulas use the static Killing-observer family. The invariant state is not $\rho_\perp$ alone but at least

$$\mathfrak{S}_\Phi = (\rho_\Phi, \widehat{q}_\mu, C), \qquad \widehat{q}_\mu = q_\mu/\rho_\Phi, \tag{16}$$

where C records local phase and null-fibre closure. Throughout, $\mathfrak{S}_\Phi$ denotes this local coarse-grained triple. The resolved causal history distribution $\mathcal{H}_A(x, k, \Gamma)$ is a separate object whose moments determine the entries and constitutive response of $\mathfrak{S}_\Phi$; it is not a fourth component of the triple.

A possible zero locus $q^2 = 0$ does not require the logarithmic chart to be continued through a singularity. The χ_Φ chart is used on a fixed-sign branch $q^2 \neq 0$; at a null seam the full variables $(q_\mu, \widehat{q}, C, \mathcal{H})$ are evolved and a neighbouring chart is attached. Thus the zero locus is a branch boundary of the scalar chart, not a divergence of the primary history state.

4. Three accelerations and distributed field momentum

The following quantities must not be conflated:

$$a^\mu_\Phi = -c^2\nabla^\mu_{\mathrm{op}}\ln\rho_\Phi, \qquad \text{physical field acceleration,} \tag{17}$$

$$\mathbf{g}_{\mathrm{coord}} = -\,\mathrm{proj}_3\,\mathbf{a}_\Phi, \qquad \text{coordinate gravitational reading,} \tag{18}$$

$$A^\mu_m = U^\nu\nabla^{\mathrm{op}}_\nu U^\mu, \qquad \text{material proper acceleration.} \tag{19}$$

In ideal free fall

$$A_m^\mu = 0, \qquad a_\Phi^\mu \neq 0. \tag{20}$$

The body feels neither an inward pull nor an outward support. The field remains physically accelerated, and the map of separations represents the body as moving inward against it. In a supported state $A_m^\mu \neq 0$ because matter is prevented from following free field transport.

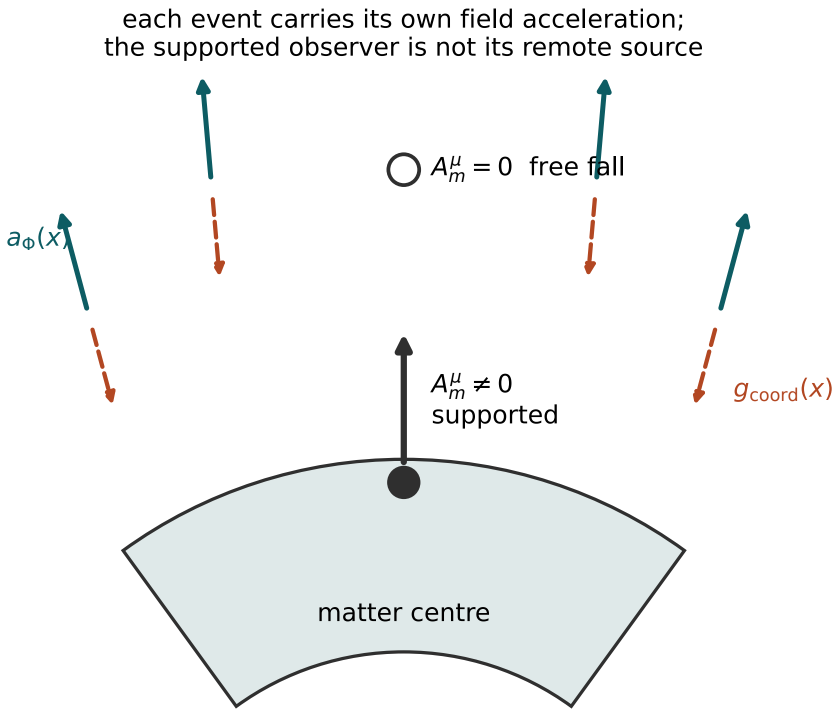

Figure 3. The three accelerations. The field carries a local outward acceleration at every event; the free faller has zero proper acceleration; the supported observer registers the force needed to prevent free transport.

The field-force picture is bath-like in the same precise sense as electromagnetic stress: energy and momentum are distributed over a field and coupled locally throughout an extended system. There need be no unique point of application. A centre of pressure is only the first moment of a distributed traction. Field momentum can be physical even when the integrated proper force on a freely falling point comparator is zero.

5. Local null-history state and exact locality

The exact state at an event is not exhausted by a scalar and finitely many of its derivatives. It is a causally accumulated distribution of null-fibre histories. Introduce

$$\mathcal{H}_A(x, k, \Gamma), \tag{21}$$

where x is the comparison event, k^μ a local null direction, Γ a transported history or holonomy class, and A collects phase, orientation, optical and closure labels.

The ontology remains strictly local. The primary equation is a transport law along each null carrier,

$$k^\mu \mathcal{D}_\mu \mathcal{H}_A + \mathcal{L}_A{}^B \mathcal{H}_B = \mathcal{S}_A[\mathcal{H}, C, T_m]. \tag{22}$$

No event acts directly across finite separation. A remote event can affect x only after information has been transported through a chain of neighbouring null updates.

Solving (22) yields a retarded representation

$$\mathcal{H}_A(x) = \mathcal{H}_A^{\mathrm{hom}}(x) + \int_{J^-(x)} \mathrm{d}V_{x'}\, G_A{}^{B'}{}_{\mathrm{ret}}(x, x')\, \mathcal{S}_{B'}(x'), \tag{23}$$

where bitensor parallel propagators compare indices only after the histories have arrived at the same event. The bilocal kernel is therefore an integrated solution representation of local transport, not action at a distance. Reflection and antipodal comparison act as endpoint holonomies on transported histories, for example $U_{\gamma_2}^{-1} R U_{\gamma_1}$, rather than as instantaneous relations between separated points.

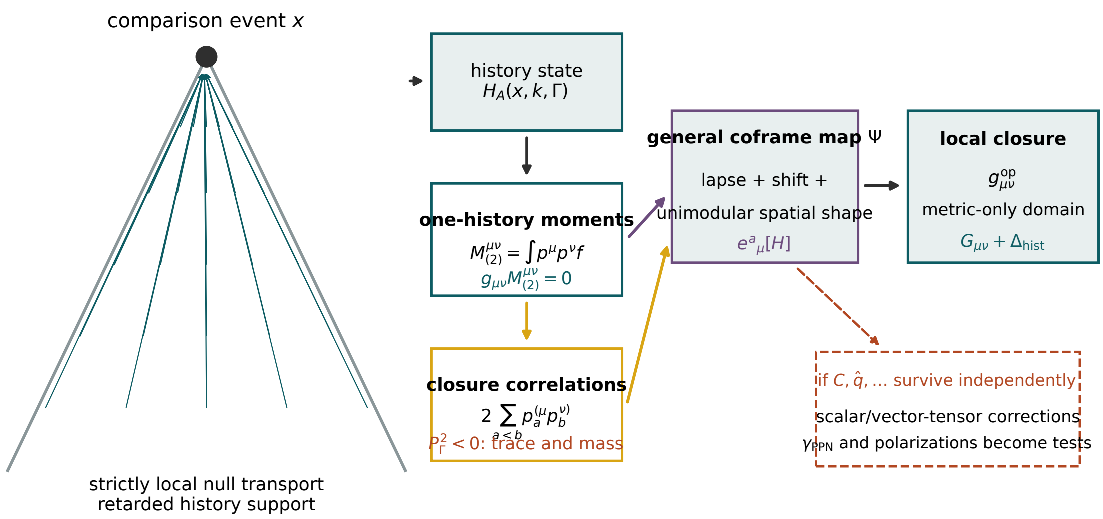

Figure 4. Exact locality with history. Null histories are transported locally into an event. Scalar, vector and tensor fields are moments of the arrived history distribution. The operational coframe and the local GR closure are later moment closures, not the primary ontology.

The causal structure itself should be derived from the principal symbol of the transport system. If

$$\det \mathcal{P}(x,p) = 0 \quad \Longrightarrow \quad \tilde{g}^{\mu\nu}(x) p_\mu p_\nu = 0, \tag{24}$$

then the operational light cone and its conformal metric class are characteristics of the field dynamics. Here $\tilde{g}_{\mu\nu}$ denotes any representative of the characteristic conformal class fixed by the principal symbol. Nullness and the trace-free identity used below are invariant under $\tilde{g}_{\mu\nu} \mapsto \Omega^2 \tilde{g}_{\mu\nu}$. The later coframe closure fixes the operational scale and selects $g^{\mathrm{op}}_{\mu\nu}$ within this class. This removes the hidden circularity in which the metric would first define ρ_Φ and then be re-derived from it.

6. Moment hierarchy and construction of the field stress

The exact history state can be reduced locally without pretending that a tensor is generated by differentiating one scalar repeatedly. Let $f_1(x,p,\Gamma)$ be the arrived one-history measure on the future null mass shell,

$$\tilde{g}_{\mu\nu} p^\mu p^\nu = 0, \qquad \mathrm{d}\Pi_x(p) = \frac{\mathrm{d}^3 p}{(2\pi\hbar)^3 p^0}, \tag{25}$$

up to the normalization fixed by the primary history action. The diagonal momentum moments are

$$M_{(n)}^{\mu_1\cdots\mu_n}(x) = \int \mathrm{d}\Gamma \int_{\mathcal{N}_x^+} \mathrm{d}\Pi_x(p)\, p^{\mu_1} \cdots p^{\mu_n} f_1(x,p,\Gamma). \tag{26}$$

In particular,

$$M_{(2)}^{\mu\nu} = \int \mathrm{d}\Gamma \int_{\mathcal{N}_x^+} \mathrm{d}\Pi_x(p)\, p^\mu p^\nu f_1. \tag{27}$$

Its trace vanishes identically,

$$\tilde{g}_{\mu\nu} M_{(2)}^{\mu\nu} = \int \mathrm{d}\Gamma \int \mathrm{d}\Pi_x(p)\, p^2 f_1 = 0. \tag{28}$$

This statement does not depend on isotropy or on whether the one-history weights are statistically correlated. Every diagonal contribution is null, so no weighting of diagonal terms can generate a trace.

Relative to an observer U^μ, the same moment decomposes as

$$M^{\mu\nu}_{(2)} = \mathcal{E}\frac{U^\mu U^\nu}{c^2} + \frac{2}{c}U^{(\mu}q^{\nu)} + p\,h^{\mu\nu} + \pi^{\mu\nu}, \tag{29}$$

with $U_\mu q^\mu = 0$, $U_\mu \pi^{\mu\nu} = 0$ and $\pi^\mu{}_\mu = 0$. With signature $(-+++)$, the trace identity gives

$$-\mathcal{E} + 3p = 0, \qquad p = \frac{\mathcal{E}}{3}. \tag{30}$$

Thus the diagonal one-history sector has the exact radiation equation of state, not merely an isotropic approximation. Every departure of the total history medium from this trace-free relation comes from non-diagonal closure correlations. Energy density, directed momentum flux, isotropic pressure and anisotropic stress are nevertheless all moments of the locally arrived history distribution.

6.1 Mass and trace from non-diagonal closure correlations

Let a closed history class Γ contain non-collinear null momenta $\{p^\mu_a\}$ and define

$$P^\mu_\Gamma = \sum_a p^\mu_a. \tag{31}$$

Then

$$P^\mu_\Gamma P^\nu_\Gamma = \sum_a p^\mu_a p^\nu_a + 2\sum_{a<b} p^{(\mu}_a p^{\nu)}_b, \tag{32}$$

$$P^2_\Gamma = 2\sum_{a<b} p_a \cdot p_b. \tag{33}$$

The diagonal sum in (32) is trace-free; the trace and invariant mass come exclusively from the cross-history terms. A closed class is massive when $P^2_\Gamma < 0$, in which case

$$m^2_\Gamma c^2 = -P^2_\Gamma = -2\sum_{a<b} p_a \cdot p_b. \tag{34}$$

Let $F_{\rm cl}(x,\Gamma)$ denote the measure on closed classes. Absorbing cycle normalization into the measure, define the non-diagonal closure tensor

$$C^{\mu\nu}_{\Phi,\rm cl} = \int \mathrm{d}\Gamma\, F_{\rm cl}(x,\Gamma)\; 2\sum_{a<b} p^{(\mu}_a p^{\nu)}_b. \tag{35}$$

The history-medium stress is therefore

$$\boxed{T^{\mu\nu}_{\Phi,\rm tot} = M^{\mu\nu}_{(2)} + C^{\mu\nu}_{\Phi,\rm cl}.} \tag{36}$$

To write the same object as a moment of timelike class totals without double counting, split the diagonal moment into open and closed-diagonal pieces,

$$M^{\mu\nu}_{(2)} = M^{\mu\nu}_{(2),\rm open} + M^{\mu\nu}_{(2),\rm cl,diag}, \qquad M^{\mu\nu}_{(2),\rm cl,diag} = \int \mathrm{d}\Gamma\, F_{\rm cl} \sum_a p^\mu_a p^\nu_a. \tag{37}$$

Then, and only with this grouping understood,

$$T^{\mu\nu}_{\Phi,\rm tot} = M^{\mu\nu}_{(2),\rm open} + \int \mathrm{d}\Gamma\, F_{\rm cl}(x,\Gamma) P^\mu_\Gamma P^\nu_\Gamma. \tag{38}$$

Equations (36) and (38) are equivalent: the closed diagonal terms occur once, inside $P^{\mu}_{\Gamma}P^{\nu}_{\Gamma}$, while $C^{\mu\nu}_{\Phi,\mathrm{cl}}$ supplies their cross terms in the first representation. Together with the microscopic knot relation (34), this is the same calculation at two resolutions: one constructs the continuum stress; the other reads the invariant mass of one closed class.

At a chosen coarse-graining scale, closed classes assigned to resolved material bodies are collected in $T_m^{\mu\nu}$, while unresolved open histories and support correlations remain in $T_{\Phi}^{\mu\nu}$. The partition is scale-dependent, but the combined momentum is not.

For comparison with geometric stiffness, set

$$\Theta^{\mu\nu}_{\Phi} = \frac{8\pi G}{c^4} T^{\mu\nu}_{\Phi,\mathrm{tot}}. \tag{39}$$

Then $[\Theta^{\mu\nu}_{\Phi}] = L^{-2}$: curvature dimension, not curvature-squared dimension. A local derivative expansion may therefore contain $(\nabla^{\mathrm{op}}\nabla^{\mathrm{op}})\chi$, $(\nabla^{\mathrm{op}}\chi)^2$, θ^2, σ^2 and ω^2, all with dimension L^{-2}.

6.2 Geometrized equilibrium and excitation stress

The same field stress must not be counted twice. Once the history-to-coframe map is fixed, write the constitutive split

$$T^{\mu\nu}_{\Phi,\mathrm{tot}} = T^{\mu\nu}_{\Phi,\mathrm{geom}} + T^{\mu\nu}_{\Phi,\mathrm{exc}}. \tag{40}$$

The equilibrium part $T^{\mu\nu}_{\Phi,\mathrm{geom}}$ is the combination of history moments already encoded in the lapse, shift and spatial coframe and therefore in $g^{\mathrm{op}}_{\mu\nu}$. It is not added again to the source side of the operational field equation. The excitation part $T^{\mu\nu}_{\Phi,\mathrm{exc}}$ is the non-equilibrium or finite-history remainder: support mismatch, finite-size multipoles, tidal loading, self-force, radiation reaction and other closure defects not absorbed by the metric-only description.

The exact local transport system conserves resolved matter plus the complete history medium. After the equilibrium part has been geometrized, the operational source equation is written

$$\mathfrak{E}^{\mu\nu}_{\Phi}[\mathcal{H}] = \frac{8\pi G}{c^4}\left(T^{\mu\nu}_{m} + T^{\mu\nu}_{\Phi,\mathrm{exc}}\right). \tag{41}$$

When the local response is expanded in the form (52), the Bianchi identity gives, in the sign convention used there,

$$\nabla^{\mathrm{op}}_{\nu}\left(T^{\mu\nu}_{m} + T^{\mu\nu}_{\Phi,\mathrm{exc}}\right) = \mathcal{J}^{\mu}_{\mathrm{hist}}, \qquad \mathcal{J}^{\mu}_{\mathrm{hist}} := \frac{c^4}{8\pi G}\left(\nabla^{\mu}_{\mathrm{op}}\Lambda_{\mathrm{eff}} + \nabla^{\mathrm{op}}_{\nu}\Delta^{\mu\nu}_{\mathrm{hist}}\right). \tag{42}$$

The separately conserved truncation

$$\nabla^{\mathrm{op}}_{\nu}\left(T^{\mu\nu}_{m} + T^{\mu\nu}_{\Phi,\mathrm{exc}}\right) = 0 \tag{43}$$

holds only when Λ_{eff} is constant and $\nabla^{\mathrm{op}}_{\nu}\Delta^{\mu\nu}_{\mathrm{hist}} = 0$ to the retained order. In general the locally transferred force density is therefore

$$Q^{\mu} = \nabla^{\mathrm{op}}_{\nu}T^{\mu\nu}_{m} = -\nabla^{\mathrm{op}}_{\nu}T^{\mu\nu}_{\Phi,\mathrm{exc}} + \mathcal{J}^{\mu}_{\mathrm{hist}}, \qquad f^{\mu}_{\mathrm{proper}} = h^{\mu}{}_{\lambda}Q^{\lambda}. \tag{44}$$

It reduces to $Q^{\mu} = -\nabla^{\mathrm{op}}_{\nu}T^{\mu\nu}_{\Phi,\mathrm{exc}}$ in the separately conserved GR truncation. Using the divergence of $T^{\mu\nu}_{\Phi,\mathrm{tot}}$ here would double-count the geometrized equilibrium field. In the point-particle GR domain $T^{\mu\nu}_{\Phi,\mathrm{exc}} \to 0$ and $\mathcal{J}^{\mu}_{\mathrm{hist}} \to 0$, so geodesic free fall carries no additional centribuoyant proper force. For extended or self-interacting systems the surviving excitation terms must reduce, on the GR domain, to the standard tidal, multipolar, self-force and radiation-reaction structures rather than to a new universal force added to Newtonian gravity [7].

6.3 From history moments to an operational coframe

The scalar exponential chart is only the static isotropic sector of a more general moment closure. Choose the Landau frame of the total second moment, so that U^μ is its future timelike eigenvector, and write

$$e^0 = Nc\,\mathrm{d}t, \qquad e^a = e^{\chi\Phi} S^a{}_b \left(\mathrm{d}x^b + \beta^b \mathrm{d}t\right), \qquad \det S = 1, \tag{45}$$

with

$$N = e^{-\chi\Phi}, \qquad \beta^a = \mathcal{B}_q\left[\frac{q^a}{\mathcal{E}}, \mathcal{H}\right], \qquad \ln S^a{}_b = \mathcal{B}_\pi\left[\frac{\pi^a{}_b}{\mathcal{E}}, \mathcal{H}\right]_{\mathrm{TF}}. \tag{46}$$

The response operators $\mathcal{B}_q$ and $\mathcal{B}_\pi$ may carry finite history; their coincidence limits are fixed by the GR embedding. The operational metric is

$$g^{\mathrm{op}}_{\mu\nu} = -e^0{}_\mu e^0{}_\nu + \delta_{ab} e^a{}_\mu e^b{}_\nu. \tag{47}$$

The shift β^a and the unimodular distortion $S^a{}_b$ are independent parts of the general map $\Psi : \mathcal{H} \mapsto e^a{}_\mu$. They cannot be generated as new degrees of freedom by first restricting the metric to one conformastatic scalar. In the static isotropic special case,

$$q^a = 0, \qquad \beta^a = 0, \qquad S^a{}_b = \delta^a{}_b, \tag{48}$$

so the independent rotational and trace-free radiative sectors vanish and (47) reduces to the exponential metric. In the general closure, the flux/normal-bundle sector supplies frame dragging and the trace-free spatial sector supplies the two tensor degrees of freedom.

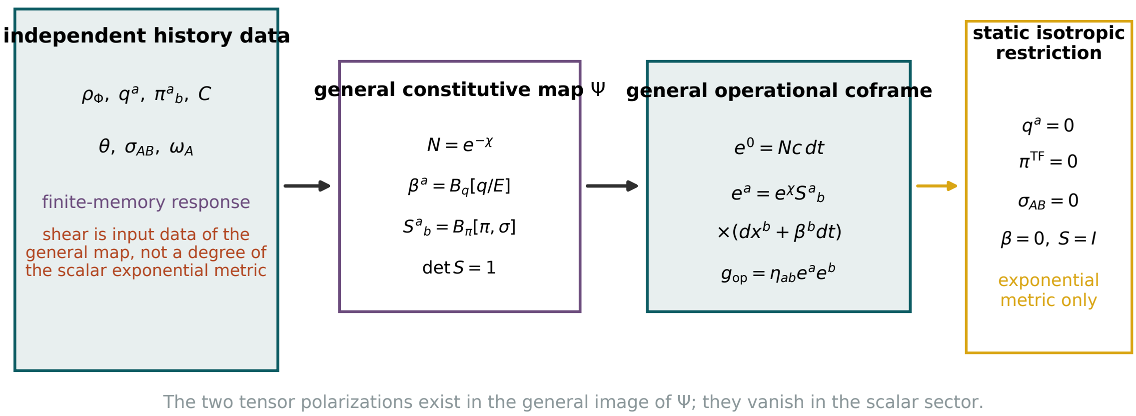

Figure 5. Moment-to-coframe closure. The scalar branch ratio fixes the lapse and isotropic scale, the momentum-flux component q^a of the second moment supplies the shift, and anisotropic stress supplies the unimodular spatial distortion. The conformastatic exponential metric is the sector $S = I$, $\beta = 0$; it does not itself contain independent shear polarizations.

7. History response, conservation and the conditional local GR limit

Four objects now have distinct roles:

1. $T^{\mu\nu}_{\Phi,\mathrm{tot}}[\mathcal{H}]$: the complete physical moment stress of the null-history medium;
2. $T^{\mu\nu}_{\Phi,\mathrm{geom}}$ and $T^{\mu\nu}_{\Phi,\mathrm{exc}}$: its geometrized equilibrium and non-equilibrium excitation parts;
3. $\mathfrak{C}^{\mu\nu}_\Phi[\mathcal{H}]$: the response functional that maps history into local clocks, separations and coframes;

4. $G^{\mu\nu}[g_{\rm op}]$: the Einstein tensor of the operational metric.

Equation (41) places only resolved matter and the excitation stress on the operational source side. The equilibrium field has already entered through $\Psi : \mathcal{H} \mapsto e^a{}_\mu \mapsto g^{\rm op}_{\mu\nu}$.

The exact response can be represented causally by a bitensor kernel,

$$\mathfrak{E}^{\mu\nu}_\Phi(x) = \int_{J^-(x)} \mathrm{d}V_{x'}\, K^{\mu\nu}{}_{\alpha'\beta'}(x,x')\mathcal{S}^{\alpha'\beta'}(x'). \tag{49}$$

A diffeomorphism-invariant action on an enlarged local state space $(e^a{}_\mu, \mathcal{H}, C, \text{matter})$ is the preferred fundamental completion. Integrating out the memory variables produces (49). Retarded mean-field equations then require an in-in/Schwinger–Keldysh prescription; inserting a retarded inverse operator directly into an ordinary in-out variational principle is not sufficient [9].

7.1 The metric-factorization condition

Let I_A denote all local coincidence invariants that can survive from the history state beside the operational metric, including C, independent components of $\widehat{q}$, preferred-frame data and local tail amplitudes. Before imposing a GR limit the leading local response has the general form

$$\mathfrak{E}^{(0)}_{\Phi,\mu\nu} = \mathcal{F}_{\mu\nu}\big[g_{\rm op}, I_A, \nabla^{\rm op} I_A, \ldots\big]. \tag{50}$$

Lovelock's theorem does *not* constrain (50) while the I_A remain independent fields. The required GR-domain assumption is the factorization

$$\boxed{\mathfrak{E}^{(0)}_{\Phi,\mu\nu}[\mathcal{H}] = \mathcal{F}_{\mu\nu}[g_{\rm op}[\mathcal{H}]], \qquad \left.\frac{\delta \mathcal{F}_{\mu\nu}}{\delta I_A}\right|_{g_{\rm op}} = 0.} \tag{51}$$

Operationally, the extra invariants must be algebraically slaved to the coframe, constant on the domain, or decoupled from matter and metric propagation at the retained order.

Only under (51), together with naturality, symmetry, divergence freedom and second-order dependence on the metric, does Lovelock uniqueness imply

$$\mathfrak{E}^{\mu\nu}_\Phi = G^{\mu\nu}[g_{\rm op}] + \Lambda_{\rm eff} g^{\mu\nu}_{\rm op} + \Delta^{\mu\nu}_{\rm hist}, \qquad \Delta^{\mu\nu}_{\rm hist} = O(\ell^2_{\rm hist}(\nabla^{\rm op})^4). \tag{52}$$

The Newtonian limit fixes the normalization of G. The theorem therefore reduces the local metric-only closure problem, but it does not eliminate the need to derive the history kernel or prove factorization [8].

If an independent closure scalar, vector or tensor survives, the correct local limit is instead

$$\mathfrak{E}^{\mu\nu}_\Phi = G^{\mu\nu} + \Lambda_{\rm eff} g^{\mu\nu}_{\rm op} + \Delta^{\mu\nu}_I + \Delta^{\mu\nu}_{\rm hist}, \tag{53}$$

with $\Delta^{\mu\nu}_I \neq 0$. This is a scalar/vector-tensor theory rather than GR. In particular, an independently coupled massless scalar generically produces a post-Newtonian gravitational slip; Brans–Dicke theory gives the familiar example $\gamma_{\rm PPN} = (1+\omega)/(2+\omega)$ [15]. Thus $\gamma_{\rm PPN} = 1$ and the Lovelock step are not separate successes: they test the same metric-factorization condition from observational and geometric directions.

7.2 Kinematic and dynamic inclusion

A genuine inclusion is both kinematic and dynamic. Let

$$\Psi : \mathcal{H} \longmapsto e^a{}_\mu[\mathcal{H}] \longmapsto g^{\rm op}_{\mu\nu}[\mathcal{H}]. \tag{54}$$

Kinematic agreement on a domain $\mathcal{D}$ requires

$$G_{\mu\nu}[\Psi(\mathcal{H})] - \frac{8\pi G}{c^4}\left(T_{m,\mu\nu} + T_{\Phi,{\rm exc},\mu\nu}\right) = O(\epsilon^{n+1}). \tag{55}$$

Dynamic inclusion requires the evolution map to commute to the same order,

$$D\Psi_{\mathcal{H}} \cdot \mathcal{V}_{\Phi}[\mathcal{H}] = \mathcal{V}_{\mathrm{GR}}[\Psi(\mathcal{H})] + O(\epsilon^{n+1}), \tag{56}$$

where $\mathcal{V}_{\Phi}$ is the null-history transport and closure flow and $\mathcal{V}_{\mathrm{GR}}$ is the characteristic Einstein evolution. This distinguishes a true GR limit from a theory that merely shares selected static line elements.

Useful validity parameters are

$$\epsilon_{\mathrm{mem}} = \frac{\ell_{\mathrm{hist}}}{L_{\mathrm{curv}}}, \qquad \epsilon_{\mathrm{cl}} = L_{\mathrm{curv}}|\nabla^{\mathrm{op}}C|, \qquad \epsilon_{\mathrm{tail}} = \frac{\|\Delta_{\mathrm{hist}}\|}{\|G[g_{\mathrm{op}}]\|}, \qquad \epsilon_{I} = \frac{\|\Delta_{I}\|}{\|G[g_{\mathrm{op}}]\|}. \tag{57}$$

The GR closure is controlled when all four are small.

8. Operational metric, PPN limit and the factor two

On the static isotropic branch the operational chart is

$$\mathrm{d}s^2_{\mathrm{op}} = -e^{-2\chi_\Phi}c^2\mathrm{d}t^2 + e^{2\chi_\Phi}\mathrm{d}\mathbf{x}^2. \tag{58}$$

The ontological order is

$$(\rho_\Phi, \widehat{q}, C, \mathcal{H}) \longrightarrow \chi_\Phi \longrightarrow g^{\mathrm{op}}_{\mu\nu} \longrightarrow \text{clock and null observables.} \tag{59}$$

The metric is the operational chart of the field, not its source.

For $|\chi_\Phi| \ll 1$,

$$g_{00} = -(1 - 2\chi_\Phi + 2\chi_\Phi^2 + \cdots), \tag{60}$$

$$g_{ij} = (1 + 2\chi_\Phi + 2\chi_\Phi^2 + \cdots)\delta_{ij}. \tag{61}$$

For comparison with the standard PPN convention, define the positive Newtonian potential $U_{\mathrm{PPN}} = c^2\chi_\Phi > 0$. The conventional signed Newtonian potential is $\Phi_N = -U_{\mathrm{PPN}} = -c^2\chi_\Phi$. Comparison with the standard PPN form then gives

$$\gamma_{\mathrm{PPN}} = 1, \qquad \beta_{\mathrm{PPN}} = 1 \tag{62}$$

for this conformastatic scalar sector.

Equation (62) is not automatically a result for the full history theory. It survives the general coframe closure only when the metric-factorization condition (51) holds and the independent history variables produce no relative slip between the clock and spatial potentials. A measured value $\gamma_{\mathrm{PPN}} \neq 1$ would therefore identify either a failure of the exponential projection or a surviving local closure mode. Conversely, the observed near-unity value constrains precisely the same extra-invariant channel that must vanish before the Lovelock argument can be used [15].

The null condition gives the optical index

$$n_{\mathrm{opt}} = e^{2\chi_\Phi}. \tag{63}$$

Therefore the operational transverse null curvature is

$$\boldsymbol{\kappa}^{\mathrm{op}}_{\mathrm{null}} = \boldsymbol{\nabla}^{\mathrm{op}}_{\perp} \ln n_{\mathrm{opt}} = 2\boldsymbol{\nabla}^{\mathrm{op}}_{\perp}\chi_\Phi = -2\boldsymbol{\kappa}^{\mathrm{field}}_{\Phi}. \tag{64}$$

The factor two is not a second force. The same field gradient is read in null transport through equal clock and spatial-scale contributions. For $\chi = m/r$, the weak-field deflection is

$$\Delta\theta = \frac{4GM}{c^2 b}. \tag{65}$$

The low-velocity orbital decomposition discussed later must not be continued to photons by substituting $v = c$ into a timelike $\gamma^2 v^2/R$ expression. The null sector is independently defined by the characteristic equation and (64).

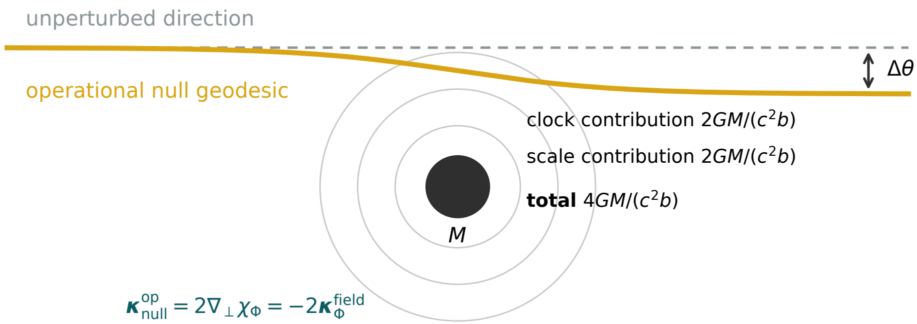

Figure 6. The null-sector factor two. Clock and spatial-scale projections contribute equally to the operational null path. Light deflection tests the field-to-chart projection; it does not generate the ontology.

9. Characteristic GR dictionary and independent tensor radiation

The natural meeting point with GR is its characteristic rather than only its ADM formulation. A degree-of-freedom distinction is essential at the outset. The shear of a chosen congruence can be computed in any fixed scalar metric, but such computed shear is not an independent metric degree of freedom. The two freely propagating tensor modes enter only through the general map $\Psi : \mathcal{H} \mapsto e^a{}_\mu$, specifically through the trace-free screen metric or the unimodular spatial coframe $S^a{}_b$. In the conformastatic scalar sector $S = I$ and $\beta = 0$, so those independent radiative modes are absent.

For a null congruence with screen basis $s_A{}^\mu$, define

$$B_{AB} = s_A{}^\mu s_B{}^\nu \nabla^{\rm op}_\nu k_\mu = \frac{1}{2}\theta\, s_{AB} + \sigma_{AB} + \omega_{AB}. \qquad (66)$$

Here θ is expansion, σ_{AB} is symmetric and trace-free, and ω_{AB} is antisymmetric. Because the screen is two-dimensional, the independent σ_{AB} supplied by the general coframe map has exactly two real components.

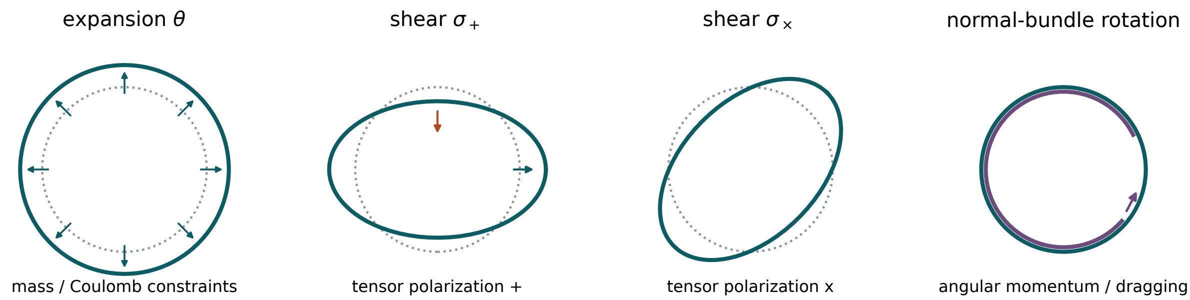

Figure 7. Optical data of the general history-to-coframe map. Expansion participates in the Coulomb and constraint sector; the two independent shear components carry the tensor polarizations; the normal-bundle connection and magnetic Weyl sector carry rotation and frame dragging. These are not extra degrees generated by the one-scalar exponential ansatz: they vanish in that special sector.

The structural dictionary is:

Null-history data	Characteristic GR reading
ρ_Φ, χ_Φ, θ and the Coulomb Weyl component	mass aspect and static/Coulomb sector; expansion alone is not mass
normal-bundle connection, angular shift and magnetic Weyl part	angular momentum, rotation and frame dragging; twist alone is not Kerr
independent trace-free shear σ_{AB}	two tensor gravitational-wave degrees of freedom
$N_{AB} = \partial_u C^{\mathrm{TF}}_{AB}$	Bondi news and radiative energy flux
C and the kernel tail	source memory, holonomy and persistent history corrections

The scalar modulation

$$\rho_\Phi = \rho_{\Phi,0} + \delta\rho_\Phi \tag{67}$$

is retained as a near-zone load, radial pump and memory-envelope variable. It is not by itself the propagating GR gravitational wave. The radiative tensor sector is

$$C^{\mathrm{TF}}_{AB}, \qquad N_{AB} = \partial_u C^{\mathrm{TF}}_{AB}, \qquad \mathcal{F}_{\mathrm{GW}} \propto N_{AB}N^{AB}. \tag{68}$$

In the metric-factorized GR domain any independent scalar breathing mode must decouple or remain below observational limits; otherwise it is an additional polarization. Multi-detector gravitational-wave observations favour the tensor sector over pure scalar or vector alternatives [12].

Bondi–Sachs and double-null formulations are especially suitable because their data are carried along null hypersurfaces. The intended embedding maps the ΦBSU transport and moment equations onto GR hypersurface constraints, shear evolution, mass and angular-momentum aspects, and supplementary conservation equations [5, 6].

10. Free orbits and the radial pump

A free circular orbit is geodesic. In the ideal point limit,

$$A^\mu_m = 0, \qquad h^\mu{}_\lambda \nabla^{\mathrm{op}}_\nu T^{\lambda\nu}_{\Phi,\mathrm{exc}} = 0. \tag{69}$$

The centribuoyant orbital term is therefore not a separate proper force on the satellite. It is a decomposition of the joint field–body momentum bookkeeping in the coordinate projection. For a static spherical field,

$$g^{(R)}_{\mathrm{coord}} + a^{(R)}_{\mathrm{cb,kin}} = 0, \tag{70}$$

while neither term alone is an accelerometer reading. Drag-free experiments test precisely this distinction: LISA Pathfinder measured residual differential nongravitational acceleration at the femto-m $\mathrm{s}^{-2}\,\mathrm{Hz}^{-1/2}$ spectral level rather than an orbital proper acceleration generated by gravity [13].

At low velocity the decomposition has the local form

$$|a_{\mathrm{cb,kin}}| \sim \frac{v^2_{\mathrm{rel}}}{R_{\mathrm{iso}}}, \qquad v_{\mathrm{rel}} \ll c, \tag{71}$$

where R_{iso} is the curvature radius of the isogradient orbit, not the field curvature radius $c^2/|a_\Phi|$. This term belongs to the operational decomposition of geodesic motion. A nonzero proper residue requires support, forcing, finite-size multipoles, tidal mismatch or self-interaction, and is carried by $T^{\mu\nu}_{\Phi,\mathrm{exc}}$.

Radial free fall and circular revolution minimise different quantities. The former minimises proper loading; the latter removes the radial pump of a single test body in a static spherical field. An elliptic orbit crosses layers periodically,

$$\frac{D\chi_\Phi}{D\tau} = \frac{\mathrm{d}r}{\mathrm{d}\tau}\partial_r\chi_\Phi \neq 0 \tag{72}$$

for most of the orbit. Its finite-mass anisotropic backreaction can drive the independent shear and Bondi news; the scalar pump supplies the source envelope. A circular binary still radiates through its rotating quadrupolar anisotropy even though a single circular test orbit has zero radial pump.

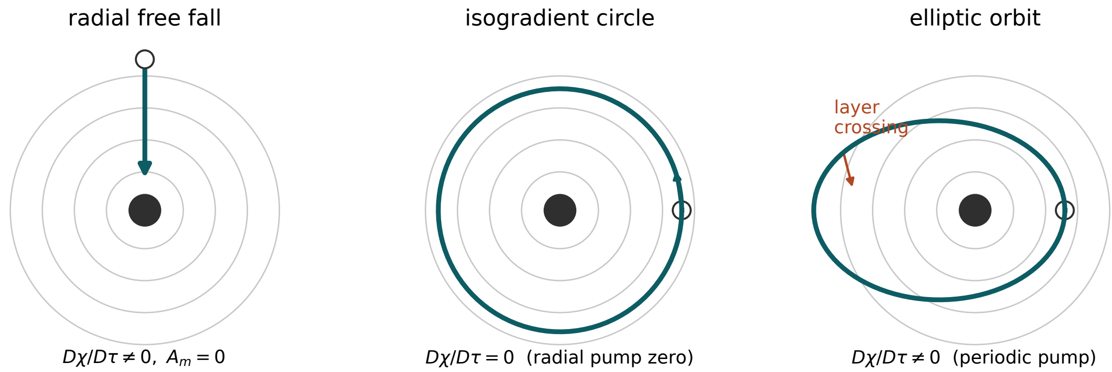

Figure 8. Three orbit classes. Radial free fall crosses field layers with zero proper acceleration; the isogradient circle removes the radial pump for a single test body; the elliptic orbit crosses layers periodically. A circular binary still radiates through the independent rotating shear sector.

11. Closure: matter as a closed null-history knot

The same field acceleration persists at microscopic scale, but its topological fate changes. Open histories continue separative transport. In a closing knot, phase, direction and momentum histories return to the same holonomic structural identity.

Each constituent momentum is null,

$$p_a^\mu p_{a\mu} = 0, \tag{73}$$

but the sum

$$P_\Gamma^\mu = \sum_a p_a^\mu \tag{74}$$

can be timelike. With signature $(- + ++)$,

$$P_\Gamma^2 = 2 \sum_{a<b} p_a \cdot p_b < 0, \qquad m_\Gamma^2 c^2 = -P_\Gamma^2. \tag{75}$$

Mass does not arise by slowing the null constituents. It is the invariant norm generated by their non-diagonal closure correlations. Equation (75) is exactly the single-knot form of the cross-history tensor $C_{\Phi,\mathrm{cl}}^{\mu\nu}$ in section 6: the diagonal second moment is trace-free at every scale, and the timelike trace appears only when distinct null histories close into one comparator.

The holonomic return is

$$\oint_\Gamma q_\mu \mathrm{d}x^\mu = 2\pi n. \tag{76}$$

If one closure cycle has characteristic time T_Γ, the proper time of the knot is

$$\tau_\Gamma = N_\Gamma T_\Gamma. \tag{77}$$

The structural identity persists while its history grows return by return. At a resolved scale such knots constitute the material stress $T_m^{\mu\nu}$; at an unresolved scale their correlations contribute to the history-medium closure.

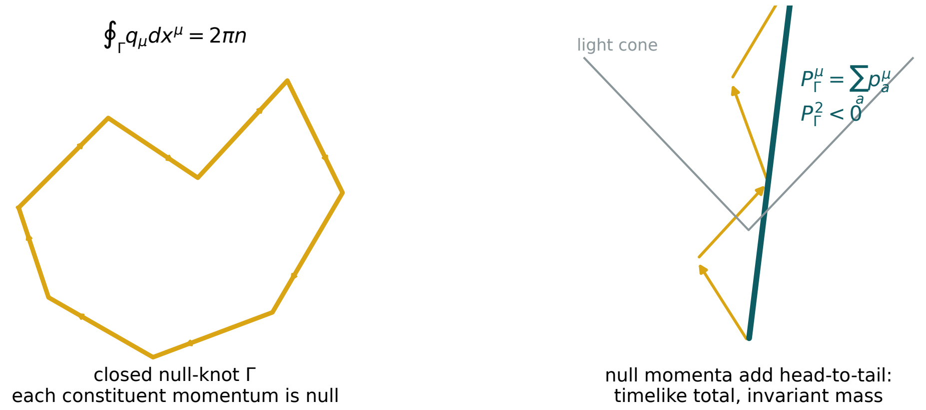

Figure 9. Closure. Every constituent remains null. The timelike total and invariant mass arise from the cross terms $2\sum_{a<b} p_a \cdot p_b$, the same non-diagonal correlations that supply the trace of the continuum stress. Ordered holonomic returns define proper-time ageing.

12. The closure continuum: matter, ambients and voids

The state triple

$$\mathfrak{S}_\Phi = (\rho_\Phi, \widehat{q}_\mu, C) \tag{78}$$

separates three regimes.

- **Matter:** strongly closed histories, high total norm and proper-time share, depleted spatial branch, timelike correlations and invariant mass.
- **Inertial ambient:** partially closed, source-anchored memory that carries support and history without closing into a free massive knot.
- **Void:** open or weakly closed history in which separative capacity remains predominantly spatial and contributes to the expansion reserve.

A schematic information budget is

$$S_{\text{write}} = S_{\text{bound}} + S_{\text{rare}}. \tag{79}$$

The distinction between matter and void is not simply high versus low one-scalar density. It is the combined orientation and closure state. This is why the same framework can support a total-density maximum in matter and an open spatial reserve in voids without identifying the two.

13. Strong-field exponential chart and the one-ended BECO closure

Here BECO denotes the buoyant exotic compact-object branch of the programme: a closed, one-ended history structure whose exterior admits the static operational chart while its interior is determined by nonlinear open–closed conversion.

The static isotropic operational metric (58) with

$$\chi(r) = \frac{m}{r}, \qquad m = \frac{GM}{c^2}, \tag{80}$$

has exact exterior identities. Its areal reading is

$$R(r) = re^{m/r}, \qquad \frac{\mathrm{d}R}{\mathrm{d}r} = e^{m/r}\left(1 - \frac{m}{r}\right), \tag{81}$$

so the map $r \mapsto R$ has a stationary fold at

$$r_* = m, \qquad R_* = em. \tag{82}$$

The proper-distance and volume integrands of the same analytic expression are

$$d\ell = e^{m/r}\,dr, \qquad dV = 4\pi r^2 e^{3m/r}\,dr. \tag{83}$$

They diverge if the formula is extended all the way to $r \to 0^+$.

13.1 What the GR wormhole comparison does and does not show

The same line element has been classified in the GR literature as a two-ended traversable wormhole [3]. That statement follows only after three extra assumptions are imposed:

1. $g^{\mathrm{op}}_{\mu\nu}$ is promoted from an operational chart to the fundamental global spacetime metric;
2. the open-branch solution $\chi = m/r$ is continued unchanged over the full interval $0 < r < \infty$;
3. both preimages of the areal radius beyond the fold are admitted as physical spacetime regions.

These assumptions define a useful comparison geometry, but they are not the ΦBSU compact-object ontology.

No-wormhole statement for the physical branch. Equality of the exterior line element with the exponential metric does not determine the global topology of the primary history state. In ΦBSU, the scalar chart is valid on an open null-history branch. When closure becomes nonperturbative, the map $\mathcal{H} \mapsto \chi \mapsto g^{\mathrm{op}}_{\mu\nu}$ changes constitutive branch. The second analytic preimage of $R(r)$ is therefore not identified with a second asymptotic universe. It is, at most, a comparison representation of internal history depth before the physical closure variables are restored.

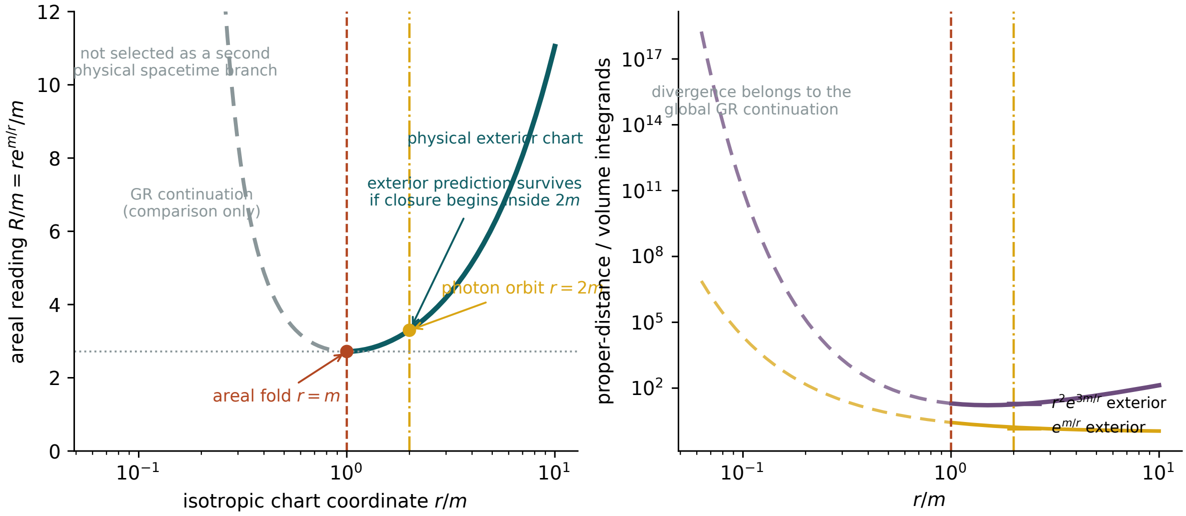

Figure 10. Exterior exponential chart and its GR continuation diagnostic. The solid branch is the physical exterior chart. The dashed continuation reproduces the mathematical branch used in the standard wormhole classification, but it is not selected as a second physical spacetime region in the ΦBSU reading.

The fold at $r = m$ is nevertheless important. It is an invariant warning that the scalar, static, one-branch map is no longer one-to-one in the areal variable. It therefore supplies a natural strong-field matching scale, but not by itself a throat or a topology.

13.2 Physical branch selection and interior matching

Let the exterior GR-like closure be valid on

$$\mathcal{D}_{\mathrm{out}} = \{r \geq r_C\}, \qquad C \simeq 0, \qquad \chi(r) = \frac{m}{r} + O(\epsilon_{\mathrm{hist}}). \tag{84}$$

At the closure layer Σ_C, the open history flux converts into closed proper-time and memory correlations. The full variables remain regular even when the scalar reciprocity chart ceases to be sufficient:

$$C\uparrow, \qquad \frac{\rho_\parallel}{\rho_\perp}\uparrow, \qquad \epsilon_{\rm mem}, \epsilon_{\rm cl} = O(1). \tag{85}$$

The physical branch selector P_+ retains one exterior and maps the complementary analytic data into the internal holonomy/memory sector. It does not create a second exterior.

A one-ended finite core is most naturally written in proper radial coordinate ℓ,

$$ds^2_{\rm in} = -N^2(\ell)c^2 dt^2 + d\ell^2 + \mathcal{R}^2(\ell) d\Omega^2, \tag{86}$$

with regular one-ended conditions

$$\mathcal{R}(0) = 0, \qquad \mathcal{R}'(0) = 1, \qquad 0 < \ell_b < \infty, \qquad V_{\rm prop} = 4\pi \int_0^{\ell_b} \mathcal{R}^2(\ell) d\ell < \infty. \tag{87}$$

A large memory depth is allowed even though no second asymptotic region exists.

The matching data are the induced two-metric, the quasilocal Killing/Noether charges, the phase flux and the null optical data. In the GR approximation a thin transition would obey an Israel-type relation [4]

$$[K_{ab} - K h_{ab}] = -\frac{8\pi G}{c^4} S^{\rm eff}_{ab}, \tag{88}$$

where $S^{\rm eff}_{ab}$ is not a new material shell but the operational surface moment of the open–closed history conversion. In a resolved transition layer, (88) is replaced by the smooth moment and transport equations.

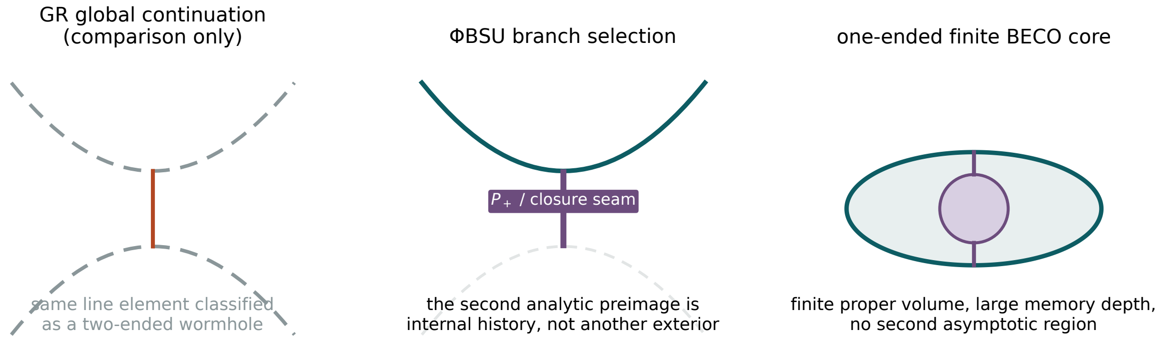

Figure 11. The GR continuation is a comparison, not the physical conclusion. The ΦBSU branch selector converts the complementary analytic preimage into internal history data, and the physical compact object is completed by a one-ended finite core.

13.3 Finite Tardis index and primary saturation

For the physical core define

$$\mathcal{T}_B = 6\sqrt{\pi}\frac{V_{\rm prop}}{A_b^{3/2}}, \qquad A_b = 4\pi\mathcal{R}^2(\ell_b). \tag{89}$$

A Euclidean ball has $\mathcal{T}_B = 1$. Values $\mathcal{T}_B > 1$ mean that the curved interior carries more proper volume than the Euclidean isoperimetric reference with the same boundary area. This is the BECO use of the Tardis concept: a boundary encloses more proper volume than the Euclidean reference, without importing the cosmological Swiss-cheese construction of Ref. [14] or requiring a second end.

For a one-ended core without a throat, $\mathcal{R}'(\ell)$ remains positive throughout the interior. A simple sufficient "stretch-Tardis" condition is

$$0 < \mathcal{R}'(\ell) \le 1 \quad (0 < \ell \le \ell_b), \qquad \mathcal{R}'(\ell) < 1 \quad \text{on an interval of nonzero length.} \tag{90}$$

Then

$$V_{\text{prop}} = 4\pi \int_0^{\mathcal{R}_b} \frac{\mathcal{R}^2}{\mathcal{R}'}\, \mathrm{d}\mathcal{R} > \frac{4\pi}{3}\mathcal{R}_b^3, \tag{91}$$

so $\mathcal{T}_B > 1$ while $\mathcal{R}'$ never vanishes. This distinguishes a one-ended stretch-Tardis interior from a throat-Tardis geometry, for which $\mathcal{R}' = 0$ at a stationary surface. The displayed condition is sufficient rather than necessary; its role is to make the intended branch explicit.

The operational gradient

$$|\nabla\chi|_{\text{op}} = e^{-\chi}|\chi'| = \frac{m}{r^2}e^{-m/r} \tag{92}$$

is already bounded in the comparison continuation. Therefore a statement that this particular norm "saturates" cannot by itself generate the finite core. Saturation must act on a primary quantity: the canonical history-flux momentum, the pre-operational coframe norm, the open–closed conversion rate, or a null-focusing invariant. With one primary scale κ_{sat}, a useful dimensionless parameter is

$$\zeta = m\kappa_{\text{sat}}. \tag{93}$$

The solution, not an independent postulate, must then determine

$$\mathcal{T}_B(\zeta), \quad r_C(\zeta), \quad b_{\text{crit}}(\zeta), \quad R_{\text{ISCO}}(\zeta) \tag{94}$$

and reveal whether one parameter is sufficient.

13.4 The GR-assigned effective source is a diagnostic

One may still ask what local stress GR would assign to the exterior operational chart. For

$$\mathrm{d}s^2 = -e^{-2\chi(r)}c^2\mathrm{d}t^2 + e^{2\chi(r)}(\mathrm{d}r^2 + r^2\mathrm{d}\Omega^2), \tag{95}$$

the Einstein-effective orthonormal density and pressures are

$$\varepsilon_{\text{eff}} = \frac{c^4}{8\pi G}e^{-2\chi}\left[-\chi'^2 - 2\chi'' - \frac{4\chi'}{r}\right], \tag{96}$$

$$p_{r,\text{eff}} = -\frac{c^4}{8\pi G}e^{-2\chi}\chi'^2, \tag{97}$$

$$p_{t,\text{eff}} = +\frac{c^4}{8\pi G}e^{-2\chi}\chi'^2. \tag{98}$$

For $\chi = m/r$ this reduces to

$$\varepsilon_{\text{eff}} = p_{r,\text{eff}} = -\mathcal{K}, \qquad p_{t,\text{eff}} = +\mathcal{K}, \qquad \mathcal{K} = \frac{c^4}{8\pi G}e^{-2m/r}\frac{m^2}{r^4}. \tag{99}$$

This is the anisotropic "antiscalar" source assigned by the global GR interpretation. In the present theory it is a diagnostic of the projection $\mathcal{H} \mapsto g^{\text{op}}_{\mu\nu}$, not the fundamental stress tensor $T_\Phi^{\mu\nu}$.

Equation (99) gives the radial effective null combination directly:

$$\varepsilon_{\text{eff}} + p_{r,\text{eff}} = -2\mathcal{K} < 0 \tag{100}$$

throughout every radius on which the exponential exterior chart is retained. The violation decays asymptotically as r^{-4}, with the additional factor $e^{-2m/r}$. If the comparison metric is globally continued through the areal fold, the fold is the point at which the flare-out condition gives this already-negative radial combination a throat interpretation; it is not the only radius where the effective NEC diagnostic is negative.

The negative local Einstein-effective density is also not the ADM/Killing mass. On a truncated exterior $r \ge r_0 > 0$ its proper-volume integral is

$$E_{\text{eff}}(r_0, \infty) = 4\pi \int_{r_0}^{\infty} \varepsilon_{\text{eff}} e^{3m/r} r^2 \mathrm{d}r = -\frac{c^4 m}{2G}\left(e^{m/r_0} - 1\right) < 0. \tag{101}$$

The positive asymptotic mass $M = c^2 m/G$ is instead a boundary charge fixed by the $1/r$ falloff. In a gravitating system it is not obtained by integrating the local effective density alone; anisotropic stresses and the gravitational boundary term are essential to the mass bookkeeping.

The physical one-ended BECO does not inherit the topology of the global comparison continuation automatically. Its effective energy conditions must be computed from the solved closure layer and core. The decisive target is stronger and cleaner:

$$\begin{aligned} T_\Phi^{\mu\nu} &: \text{ positive kinetic matrix and causal transport,} \\ G^{\mu\nu}[g_{\mathrm{op}}] &: \text{ effective negative pressure may appear in the closure projection.} \end{aligned} \tag{102}$$

Thus the external GR comparison identifies where history corrections are needed; it does not establish exotic fundamental matter or a wormhole topology.

13.5 Quasilocal Archimedes balance and stability

A vector integral such as $\int_{\mathcal{B}} T^{\mu\nu} n_\nu \mathrm{d}\Sigma$ is not generally a well-defined global momentum because it adds tangent vectors at different points. In a static spacetime the timelike Killing vector ξ^μ supplies a well-defined current

$$J_\xi^\mu = T^{\mu\nu}\xi_\nu, \qquad \nabla_\mu^{\mathrm{op}} J_\xi^\mu = 0, \tag{103}$$

and a scalar quasilocal energy

$$E_\xi[\Sigma] = \int_\Sigma T_{\mu\nu}\xi^\mu n^\nu \mathrm{d}V. \tag{104}$$

For dynamical or rotating systems, Brown–York or rigid-quasilocal-frame boundary stress is the appropriate replacement [10, 11]. This is the four-dimensional Archimedes form: distributed field traction is integrated over a worldtube, and only its uncancelled multipoles become proper force, torque or tidal load.

A finite BECO solution should satisfy four conditions:

1. **Exterior closure:** $\chi \to m/r$ in the open, low-memory region.
2. **One-ended finite Tardis core:** $1 < \mathcal{T}_B < \infty$, derived from the nonlinear history closure with no second asymptotic region.
3. **Effective exoticity without a fundamental ghost:** any negative operational pressure or defocusing is produced by the history-to-chart projection, while the primary kinetic matrix is positive and the transport system is hyperbolic and causal.
4. **Quasilocal and dynamical stability:** the constrained energy is a local minimum, the coupled perturbation spectrum has no exponentially growing modes, and all tidal invariants remain finite.

13.6 Strong-field observables of the exterior branch

If the exterior exponential chart remains valid down to the relevant radii, it gives

$$r_{\mathrm{ph}} = 2m, \qquad R_{\mathrm{ph}} = 2\sqrt{e}\,m, \tag{105}$$

$$b_{\mathrm{crit}} = 2em \simeq 5.4366m, \tag{106}$$

$$r_{\mathrm{ISCO}} = (3+\sqrt{5})m, \qquad R_{\mathrm{ISCO}} \simeq 6.33794m. \tag{107}$$

Schwarzschild has $b_{\mathrm{crit}} = 3\sqrt{3}m \simeq 5.1962m$, so the exponential critical impact parameter is about 4.63% larger.

Exterior photon-ring robustness. The areal-map fold is at $r_* = m$, $R_* = em \simeq 2.718m$, whereas the photon orbit is at $r_{\mathrm{ph}} = 2m$, $R_{\mathrm{ph}} = 2\sqrt{e}\,m \simeq 3.297m$. The photon orbit therefore lies outside the fold. The prediction $b_{\mathrm{crit}} = 2em$ survives every one-ended BECO completion whose nonlinear closure radius satisfies $r_C < 2m$ and whose exterior characteristic map remains exponential. It does not rely on the two-ended GR continuation.

A dark shadow is not guaranteed by the metric alone. It requires an inner boundary condition that absorbs, decoheres or strongly redshifts the transmitted null histories. A reflective or emissive BECO core can instead produce additional rings, echoes or central brightness. The closure radius is therefore observational: if $r_C \geq 2m$, even the critical ring changes; if $r_C < 2m$, the exterior ring is retained while the central response distinguishes the core.

14. The characteristic GR embedding programme

The precise GR inclusion statement can now be organised as follows.

1. **Primary state:** define $\mathcal{H}_A(x, k, \Gamma)$, its local transport, closure and holonomy equations, and the primary norm (4).
2. **Moment hierarchy:** derive $M^{(0)}$, $M_{(1)}$, $M_{(2)}$ and closed-history correlations; fix the measure and construct $T^{\mu\nu}_{\Phi}$ by (36).
3. **Characteristic map:** derive the principal symbol, the operational coframe, the optical variables (θ, σ, ω) and the map $\Psi : \mathcal{H} \mapsto g_{\rm op}$.
4. **Causal variational structure:** obtain the transport and moment equations from a local enlarged-state action; derive retarded mean-field equations only after the memory variables are integrated out.
5. **Metric factorization and local Einstein closure:** prove (51); only then use Lovelock uniqueness in (52). Show simultaneously that independent closure modes produce no PPN slip, or retain and test the resulting scalar/vector-tensor sector.
6. **Dynamic characteristic equivalence:** establish (56) against Bondi-Sachs or double-null evolution, including the two shear polarizations and the correct supplementary conservation laws.
7. **Strong-field completion:** solve the spherical BECO core, then rotation, shear perturbations, stability, tidal response, photon rings and ringdown.

This order keeps the tensor continuum in its proper role. GR is neither rejected nor assumed as fundamental. It is the local, short-memory, second-moment closure of a separative history theory, while the higher moments and finite memory retain the distinctive ΦBSU corrections.

15. Domain of validity, derivation tasks and falsification

Result or structural consequence established here	Constitutive or nonlinear derivation still required
Field, coordinate and material proper accelerations are separated event-locally	full material coupling for arbitrary extended bodies
ρ_Φ **and** $\rho_\perp$ **give consistent opposite profiles on the static observer branch**	dynamical derivation and domain of the reciprocity relation
Every diagonal null second moment is trace-free; mass and trace arise from cross-history closure terms	normalized history measure and open–closed conversion operator
$T_{\Phi,\mathrm{geom}}$ **is encoded in the coframe while only** $T_{\Phi,\mathrm{exc}}$ **remains on the source side**	derivation of the constitutive projector and its reduction to GR self-force, tidal and radiative terms
Retarded history dependence is the integrated representation of local null transport	causal enlarged-state action and in-in reduction
Lovelock applies only after metric factorization; $\gamma_{\mathrm{PPN}} = 1$ **tests the same condition**	proof that C and other local invariants are slaved, constant or decoupled on the GR domain
The general coframe contains independent shift and trace-free spatial sectors; the scalar exponential metric does not	source map from scalar loading and anisotropic moments to Bondi news
The photon orbit $r = 2m$ **lies outside the areal fold** $r = m$	finite, stable one-ended BECO core and its boundary response
Quasilocal momentum requires Killing or boundary-stress data	rotating and nonstationary BECO conservation and stability

The principal falsification channels are direct.

1. A post-Newtonian slip $\gamma_{\mathrm{PPN}} \neq 1$ or an unsuppressed extra polarization would falsify metric factorization on the claimed GR domain.
2. A universal proper acceleration on an ideal freely orbiting point body would contradict the geometrized/excitation split and geodesic limit.
3. Failure of the shear sector to reproduce tensor Bondi news would invalidate the proposed characteristic embedding.
4. If nonlinear closure begins inside $r = 2m$, an exterior critical ring incompatible with $b_{\mathrm{crit}} = 2em$ would falsify the exponential exterior branch independently of any wormhole interpretation.
5. A one-ended BECO completion that necessarily carries a fundamental ghost, a divergent tidal invariant or an unstable mode would invalidate the strong-field branch.

16. Summary

The construction can be stated in one chain:

$$\boxed{\begin{array}{c}\text{local null-history transport} \longrightarrow \text{diagonal moments and closure cross-correlations} \longrightarrow T^{\mu\nu}_{\Phi,\mathrm{tot}},\ e^a{}_\mu,\ g^{\mathrm{op}}_{\mu\nu} \\ \longrightarrow \text{metric-factorized Einstein closure} \quad + \quad \text{excitation and finite-history corrections.}\end{array}} \tag{108}$$

The physical field acceleration is outward and belongs to the c-transported null-history medium. The inward gravitational acceleration is the coordinate shadow of the depleted spatial branch. A freely falling or freely orbiting point body reads zero proper acceleration, while distributed field momentum remains physical.

The field stress is not a tensor guessed from one scalar. Its diagonal second moment carries energy, flux, pressure and anisotropic stress but is identically trace-free. Invariant mass and the stress trace arise from non-diagonal correlations when distinct null histories close into a timelike total. Once the coframe is reconstructed, the equilibrium part of this stress is geometrized; only the excitation remainder can appear as an additional source or proper-force residue. This removes the possibility of interpreting centribuoyancy as a new universal force added on top of Newtonian gravity.

GR is a conditional local closure. The Lovelock step is valid only if the coincidence response factors through the operational metric and no independent closure invariant remains. The same condition is tested observationally by $\gamma_{\mathrm{PPN}} = 1$ and by the absence of extra gravitational-wave polarizations. The general coframe carries shift, rotation and an independent trace-free spatial sector; the scalar exponential metric is the special case in which those degrees vanish.

The exponential chart supplies a precise static exterior. Its global two-ended GR continuation is a useful comparison but does not fix the physical topology. A BECO is the one-ended nonlinear history closure of that exterior. Because the exterior photon orbit at $r = 2m$ lies outside the areal fold at $r = m$, the critical impact parameter $b_{\mathrm{crit}} = 2em$ is a robust exterior prediction whenever the core transition occurs inside the photon orbit. The remaining strong-field task is to derive a finite, stable core whose effective defocusing follows from orientation and closure while the primary history dynamics remains causal and ghost-free.

A. Static exponential identities and the comparison continuation

For reference, with

$$\mathrm{d}s^2 = -e^{-2\chi}c^2\mathrm{d}t^2 + e^{2\chi}(\mathrm{d}r^2 + r^2\mathrm{d}\Omega^2), \tag{109}$$

the areal reading and proper radial derivative are

$$R = re^{\chi}, \qquad \frac{\mathrm{d}R}{\mathrm{d}\ell} = 1 + r\chi', \qquad \mathrm{d}\ell = e^{\chi}\mathrm{d}r. \tag{110}$$

An areal stationary surface satisfies

$$1 + r\chi' = 0. \tag{111}$$

If the metric is promoted to a global GR geometry, the additional flare-out condition is

$$\frac{\mathrm{d}^2R}{\mathrm{d}\ell^2} = e^{-\chi}(\chi' + r\chi'') > 0, \tag{112}$$

and the surface is then interpreted as a wormhole throat. For $\chi = m/r$, the stationary surface is $r = m$, $R = em$. In the physical ΦBSU branch this calculation is retained as a comparison diagnostic; the topology beyond the stationary surface is fixed by the history-closure solution, not by analytic continuation of the scalar chart. The optical index is $n = e^{2\chi}$, and circular null motion occurs at the extremum of $e^{-4\chi}/r^2$; for $\chi = m/r$ this is $r = 2m$ with $b_{\mathrm{crit}} = 2em$.

B. Conditional local-GR proposition

Proposition. Let a local history theory define a diffeomorphism-covariant response $\mathfrak{E}_{\mu\nu}[\mathcal{H}]$ and an operational metric $g^{\mathrm{op}}_{\mu\nu}[\mathcal{H}]$. Assume on a domain $\mathcal{D}$ that (i) the memory length is small compared with the curvature scale; (ii) closure gradients and finite-tail corrections are small; (iii) the leading coincidence response factors through the operational metric as in (51), so that no independent history invariant survives beside it; and (iv) the resulting metric tensor is natural, symmetric, divergence-free and at most second order. Then in four dimensions

$$\mathfrak{E}_{\mu\nu} = aG_{\mu\nu}[g_{\mathrm{op}}] + bg^{\mathrm{op}}_{\mu\nu} + O(\ell^2_{\mathrm{hist}}(\nabla^{\mathrm{op}})^4). \tag{113}$$

The Newtonian limit fixes $a = 1$ in the normalization of (41); b is the effective cosmological term. Dynamic GR inclusion additionally requires (56). If condition (iii) fails, Lovelock's conclusion does not apply and the surviving $\Delta^{\mu\nu}_{I}$ must be treated and tested as an additional scalar/vector-tensor sector.

The proposition does not derive the history kernel or prove factorization. It isolates the theorem-sized burden: construct the primary local theory, derive the constitutive coframe map, prove that all independent local history variables decouple or become metric data on $\mathcal{D}$, and demonstrate dynamic characteristic equivalence. The equality $\gamma_{\mathrm{PPN}} = 1$ is an observational test of the same factorization assumption.

References

[1] E. Sakkinen, "ΦBSU - Buoyant Separverse Unification - Field Theory, Part I: Completing Relativity," preprint, updated 2026.

[2] E. Sakkinen, "A New Reflection-Graded Hypersymmetry on $M_4 \times K_2$," preprint, updated 2026.

[3] P. Boonserm, T. Ngampitipan, A. Simpson and M. Visser, "The exponential metric represents a traversable wormhole," *Phys. Rev. D* **98**, 084048 (2018), arXiv:1805.03781.

[4] W. Israel, "Singular hypersurfaces and thin shells in general relativity," *Nuovo Cimento B* **44**, 1-14 (1966); erratum **48**, 463 (1967).

[5] T. Mädler and J. Winicour, "Bondi-Sachs Formalism," *Scholarpedia* **11**, 33528 (2016), arXiv:1609.01731.

[6] M. Mars and G. Sánchez-Pérez, "Double Null Data and the Characteristic Problem in General Relativity," arXiv:2205.15267.

[7] E. Poisson, A. Pound and I. Vega, "The motion of point particles in curved spacetime," *Living Rev. Relativ.* **14**, 7 (2011), arXiv:1102.0529.

[8] A. Navarro and J. Navarro, "Lovelock's theorem revisited," arXiv:1005.2386.

[9] A. O. Barvinsky, "Dark energy and dark matter from nonlocal ghost-free gravity theory," *Phys. Lett. B* **710**, 12-16 (2012), arXiv:1112.4340.

[10] R. J. Epp, R. B. Mann and P. L. McGrath, "Momentum in General Relativity: Local versus Quasilocal Conservation Laws," arXiv:1306.5500.

[11] P. L. McGrath, "Rigid Quasilocal Frames," PhD thesis, University of Waterloo (2014), arXiv:1402.1443.

[12] B. P. Abbott et al. (LIGO Scientific and Virgo Collaborations), "GW170814: A Three-Detector Observation of Gravitational Waves from a Binary Black Hole Coalescence," *Phys. Rev. Lett.* **119**, 141101 (2017), arXiv:1709.09660.

[13] M. Armano et al., "New LISA Pathfinder Results down to 20 μHz," *Phys. Rev. Lett.* **120**, 061101 (2018), doi:10.1103/PhysRevLett.120.061101.

[14] M. Lavinto, S. Räsänen and S. J. Szybka, "Average expansion rate and light propagation in a cosmological Tardis spacetime," *JCAP* **12**, 051 (2013), arXiv:1308.6731.

[15] C. M. Will, "The confrontation between general relativity and experiment," *Living Rev. Relativ.* **17**, 4 (2014).